Contents

1. Theoretical Background

This chapter provides a short introduction into Josephson junctions and their role in dc-SQUIDs[1], which will be the main focus of this thesis. We start with a brief overview on macroscopic quantum phenomena such as the Josephson effect and explain the general working principle of superconductor-isolator-superconductor (SIS) tunnel contacts, followed by a summary of their basic properties. They form the theoretical framework to describe SQUIDs, which are developed in this group and optimized within the scope of this thesis. Lastly, we will take a closer look into their resonance behavior and investigate different solution approaches.

1.1 Josephson junctions

The *Josephson junctions* named after Brian D. Josephson consist of two identical superconductors weakly coupled to each other. In the case of the junctions produced in this working group, such coupling is realized through a few nm thin insulating layer between the superconducting electrodes. Consequently, they are referred to as SIS (Superconductor-Insulator-Superconductor) junctions. The resulting trilayer structure typically consists of Nb/Al-AlO_x/Nb, with niobium being used for the superconductors and the insulating layer being provided by the aluminum oxide. A schematic structure is shown in figure 1.1. By connecting the tunnel junction to a current source they exhibit a non-trivial current-voltage behavior, which will be covered in the following.

1.1.1 Josephson effect

According to the BCS theory developed by Bardeen, Cooper and Schrieffer in 1957 [Bar57], electrons in a superconductor form pairs below a material dependent critical temperature T_c. These composite particles are also referred to as *Cooper pairs* and they represent the superconducting charge carriers with twice the mass and charge of a single electron. Their dissipationless flow causes the current to have zero resistance, which is alongside the Meissner-Ochsenfeld effect [Mei33] the most characteristic feature of a superconductor. The latter describes magnetic field expulsion below T_c, provided the external magnetic field is smaller than a critical field B_c. Further details on the microscopic theory of superconductivity can be found in [Bar57] and

[1] **d**irect **c**urrent **S**uperconducting **QU**antum **I**nterference **D**evice

[Gin50].

If at $T < 4\,\mathrm{K}$ an external current source is connected to a Josephson junction, a supercurrent will flow despite the tunnel barrier, implying the tunneling of Cooper pairs as niobium is predominantly superconducting at these temperatures ($T_\mathrm{c} = 9.3\,\mathrm{K}$). Since the tunneling probability of an individual electron is approximately $p = 10^{-4}$ [Gro16], a much lower probability is to be expected for a Cooper pair consisting of two electrons. However, Josephson predicted that the tunneling behavior of Cooper pairs and individual conduction electrons must be the same. This is justified by the so-called *Macroscopic Quantum Model*, formulated by Fritz London in 1953.

The main focus here lies on the quantum mechanical phase θ. On one hand, the distance between both electrons in a Cooper pair is approximately 10 to 1000 nm which is significantly larger than the spacing between Cooper pairs, resulting in strongly overlapping wave functions. On the other hand, Cooper pairs have to obey Bose-Einstein statistics due to their total spin of 0. Thus, all Cooper pairs share the same ground state, and as a consequence, the energies and temporal evolutions of the phases are equal. These two effects lead to what is known as *phase-lock*. The phases of neighboring pairs synchronize such that this quantum mechanical property now holds on a macroscopic scale. This gives rise to a macroscopic wave function

$$\Psi(\mathbf{r}, t) = \Psi_0(\mathbf{r}, t)e^{i\theta(\mathbf{r},t)} \quad , \tag{1.1}$$

which describes all charge carriers of the superconductor. Here, the charge carrier density is given by $|\Psi_0(\mathbf{r}, t)|^2 = n_\mathrm{s}$. t denotes the time and $\mathbf{r}$ represents the position of the Cooper pair ensemble. As a result of sharing the same phase, both electrons of a Cooper pair consequently possess the same tunneling probability as an individual

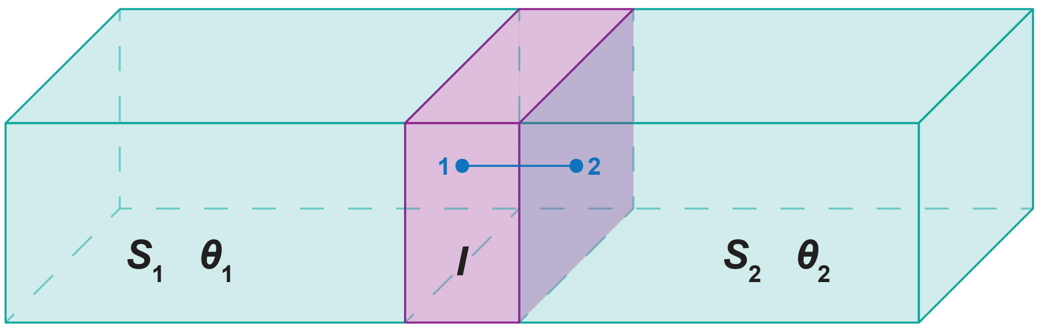

Figure 1.1: Schematic of a Josephson (SIS) junction. Both superconducting electrodes $\boldsymbol{S_1}$ and $\boldsymbol{S_2}$ are weakly coupled with each other through a thin tunnel barrier $\boldsymbol{I}$. $\boldsymbol{\theta_1}$ and $\boldsymbol{\theta_2}$ represent the macroscopic phases of each superconductor.

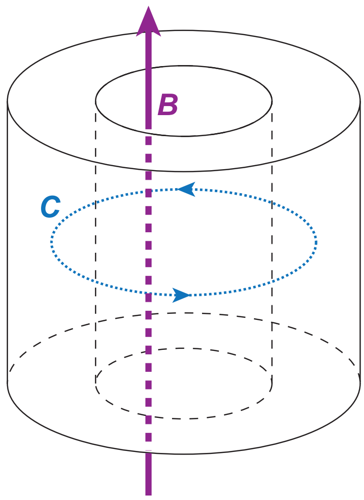

Figure 1.2: Superconducting ring-shaped cylinder threaded by an external magnetic field. By applying the field at low temperatures, shielding currents arise to expel the field from the superconductor. Upon turning off the external field the shielding currents will remain due to the lack of resistance, causing magnetic flux to be trapped. The dotted blue path C is situated at the center of the cylinder wall, which we assume to be current-free due to the London penetration depth λ_{L} being much smaller than the thickness of the cylinder wall.

electron, enabling the supercurrent. This coherence phenomenon is referred to as the *Josephson effect* [Jos62]. Another significant consequence of the macroscopic quantum model is flux quantization. Together with the Josephson effect, this forms the basis for Josephson junctions and their applications.

Flux quantization is derived through the capture of an external magnetic flux within a superconducting cylinder (see figure 1.2). The wave function must remain unchanged after circumnavigating the cylinder due to $e^{i\theta} = e^{i\theta+2\pi n}$. As a result, upon integrating along the current-free center of the cylinder wall (path C), the following equation holds for the captured flux

$$\Phi = \frac{h}{q_{\mathrm{s}}} n = \frac{h}{2e} n \equiv \Phi_0 n \quad . \tag{1.2}$$

Here, $n \in \mathbb{Z}$ and $\Phi_0 = 2.07 \times 10^{-15}\,\mathrm{T\,m^2}$ [Tie21] represents the so-called magnetic flux quantum. The captured flux is thus quantized, a consequence solely arising from the macroscopic nature of the phase. This quantity plays a crucial role in the theoretical description of Josephson junctions.

The current and voltage behavior in a SIS junction is described by the *Josephson equations*. Crucial to this description is a critical current I_{c} that is linearly proportional to the applied current I, which marks the boundary between two operational modes. Additionally, due to the macroscopic nature of the phase, I oscillates with the gauge-invariant phase difference φ, leading to the **first Josephson equation** [Jos65]

$$I_{\mathrm{s}} = I_{\mathrm{c}} \sin(\varphi) \quad . \tag{1.3}$$

I_c is proportional to the coupling strength κ, which describes the overlap of the wave functions Ψ_1 and Ψ_2 within the insulating layer. The relationship is given by

$$I_c = \frac{4e\kappa V n_s}{\hbar} \quad , \tag{1.4}$$

where V represents the volume of the superconducting electrode and e denotes the elementary charge of an electron. We assume that the Cooper pair density n_s of the two superconductors S_1 and S_2 is identical, meaning $n_{s1} = n_{s2} = n_s$.

The gauge-invariant phase difference refers to the phases θ_1 and θ_2 of the respective electrodes at the boundary of the insulating layer (positions 1 and 2, see figure 1.1). Taking into account possible external electromagnetic fields within the barrier, the general form using the vector potential $\mathbf{A}$ is given by [Gro16]

$$\varphi(\mathbf{r}, t) = \theta_2(\mathbf{r}, t) - \theta_1(\mathbf{r}, t) - \frac{2\pi}{\Phi_0} \int_1^2 \mathbf{A}(\mathbf{r}, t) \cdot \mathrm{d}\mathbf{l} \quad . \tag{1.5}$$

Assuming a constant supercurrent density J_s across the junction, taking the time derivative of equation (1.5) yields the **second Josephson equation** [Jos65]

$$\frac{\partial \varphi}{\partial t} = \frac{2\pi}{\Phi_0} V \quad . \tag{1.6}$$

The first operating mode describes the case for $I < I_c$. Here, the entire injected current is carried by Cooper pairs, so $I = I_s = \text{const}$. As a result, φ is temporally constant, which, according to equation (1.6), leads to $V = 0$. This voltage-free state is known as the *dc Josephson effect*.

For $I > I_c$ however, Cooper pairs begin to break up such that a portion of the current needs to be carried by quasiparticles, which will then lead to a voltage drop V. According to the second Josephson equation, the phase φ becomes time dependent, and after integration one obtains

$$\varphi = \frac{2\pi}{\Phi_0} V t + \varphi_0 = w_J t + \varphi_0 \quad \text{with} \quad w_J = \frac{2\pi}{\Phi_0} V \quad . \tag{1.7}$$

Thus, if we insert equation (1.7) into equation (1.3), we observe that the current I_s oscillates with the *Josephson frequency* $\frac{f_J}{V} = \frac{w_J}{2\pi V} = \frac{1}{\Phi_0} \approx 483.6\,\frac{\mathrm{MHz}}{\mu\mathrm{V}}$. Accordingly, this phenomenon is referred to as the *ac Josephson effect*.

1.1.2 Josephson Junctions in a Magnetic Field

To motivate the structure of a dc-SQUID, it is essential to first investigate the current behavior of an extended Josephson junction in the presence of an external magnetic field. So far, all previous formulae apply for point-like junctions, assuming a spatially constant phase difference φ and Josephson current density J_s across the junction area. This is not the case for three-dimensional (extended) junctions with a length L and width W. The *Josephson penetration depth* λ_J is a quantity used to classify an extended junction as short $(\mathrm{W}, \mathrm{L} \leq \lambda_J)$ or long $(\mathrm{W}, \mathrm{L} \geq \lambda_J)$ and is defined as

$$\lambda_J = \sqrt{\frac{\Phi_0}{2\pi\mu_0 J_c t_B}} \quad . \tag{1.8}$$

Here, the magnetic thickness is defined as $t_B = d + \lambda_{L,1} + \lambda_{L,2}$. It describes how far an external magnetic field penetrates both superconducting electrodes if applied parallel

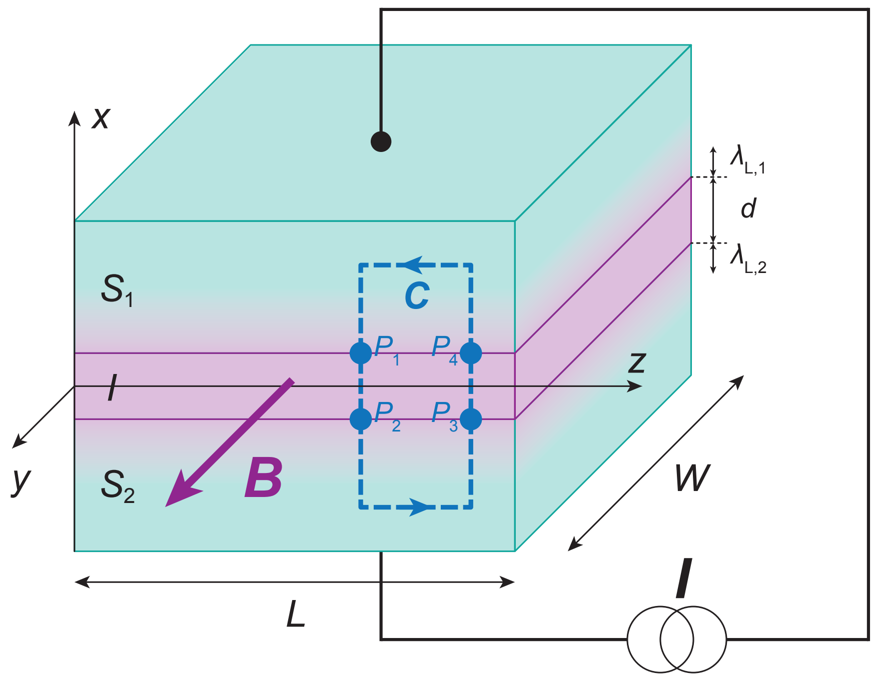

Figure 1.3: Short Josephson junction connected to a current source in the presence of an external B-field in y-direction, parallel to the junction area. Inside the electrodes the magnetic field decays exponentially according to the London penetration depths $\lambda_{L,1}$ and $\lambda_{L,2}$, visually shown by the purple color gradient. The closed contour C is used to derive expressions for the spatially dependent phase difference φ and current density J_s.

to the junction area, as depicted in figure 1.3. $\lambda_{\mathrm{L},1}$ and $\lambda_{\mathrm{L},2}$ are the respective London penetration depths and $J_{\mathrm{c}} = \frac{I_{\mathrm{c}}}{WL}$ the critical current density. This distinction is needed to determine whether the magnetic self-field generated by the supercurrent is negligible in comparison to the external field (short junctions) or not (long junctions). Within the scope of this thesis, only short junctions are used.

To analyze the current and phase distribution of such a junction we consider the setup shown in figure 1.3. A short junction is connected to a current source and is penetrated by an external B-field in y-direction, parallel to the junction area. Now, obtaining an expression for the phase requires a similar approach as the calculation for the quantized flux, where we assumed that the phase changes by $2\pi n$ around a closed loop. Here, we again integrate over a closed contour C, with the points $P_1 - P_4$ marking the transitions between superconductor and isolator. Using equation 1.5, we find

$$\frac{\partial \varphi}{\partial z} = \frac{2\pi}{\Phi_0} B_{\mathrm{y}} t_{\mathrm{B}} \quad \text{and} \quad \frac{\partial \varphi}{\partial y} = -\frac{2\pi}{\Phi_0} B_{\mathrm{z}} t_{\mathrm{B}} \quad . \tag{1.9}$$

In this experiment, however, the magnetic field points in y-direction only, meaning φ will only vary along the z-axis. Integrating the first expression in equation 1.9 then leads to

$$\varphi(z) = \frac{2\pi}{\Phi_0} B_{\mathrm{y}} t_{\mathrm{B}} z + \varphi_0 \quad . \tag{1.10}$$

Here, the integration constant φ_0 represents the phase difference for the case $z = 0$. Inserting equation 1.10 into the first Josephson equation and using $J_{\mathrm{s}} = \frac{I_{\mathrm{s}}}{WL}$ gives

$$J_{\mathrm{s}}(y, z, t) = J_{\mathrm{c}}(y, z) \sin(kz + \varphi_0) \quad \text{with} \quad k = \frac{2\pi}{\Phi_0} B_{\mathrm{y}} t_{\mathrm{B}} \quad . \tag{1.11}$$

If we now assume the critical current density J_{c} to be constant across the junction area, we can integrate equation 1.11 to get a flux-dependent maximum Josephson current

$$I_{\mathrm{s}}^{\mathrm{m}}(\Phi) = I_{\mathrm{c}} \left| \frac{\sin(\frac{kL}{2})}{\frac{kL}{2}} \right| = I_{\mathrm{c}} \left| \frac{\sin(\frac{\pi\Phi}{\Phi_0})}{\frac{\pi\Phi}{\Phi_0}} \right| \quad . \tag{1.12}$$

This expression describes the so-called Fraunhofer diffraction pattern, shown in figure 1.4. The result resembles the single slit experiment, where the same pattern is found for the light intensity behind the slit. Here, the analogy works by considering the integral of the critical current density J_{c} as a transmission function which is constant inside the junction and zero outside.

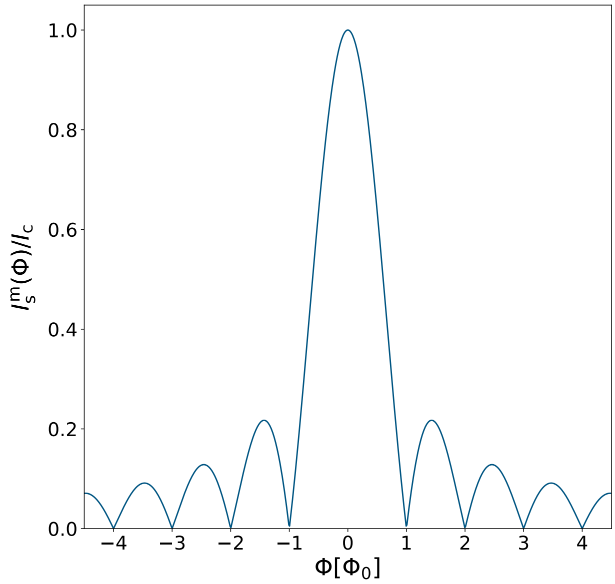

Figure 1.4: Normalized flux-dependent maximum Josephson current $I_{\mathrm{s}}^{\mathrm{m}}(\Phi)$ showing a Fraunhofer pattern. It modulates with the flux quantum Φ_0, peaking at $\Phi = 0$ with subsequent maxima at $\Phi = \pm(\frac{3}{2} + n)\Phi_0$ with $n \in \mathbb{N}_0$. For $\Phi = \pm(n + 1)\Phi_0$ the total net current is zero.

1.1.3 RCSJ Model

Until now, we investigated the current-voltage behavior under the assumption of $I < I_{\mathrm{c}}$, staying in the so-called zero-voltage state. In this regime, only the dc Josephson effect applies as discussed in subchapter 1.1.1. Switching to the voltage stage, i.e. $I > I_{\mathrm{c}}$, Cooper pairs start breaking up into quasiparticles if the electric energy eV or thermal energy $k_{\mathrm{B}}T$ exceeds the sum of both electrodes' gap energies $\Delta_1 + \Delta_2$. Consequently, at the *gap-voltage*

$$V_{\mathrm{g}} = \frac{\Delta_1(T) + \Delta_2(T)}{e} \tag{1.13}$$

quasiparticles start to cross the tunnel barrier resulting in a steep rise of a resistive normal current I_{N}. Under a current source, the condition $I = I_{\mathrm{s}} + I_{\mathrm{N}}$ must be constantly fulfilled. This results in an oscillating normal current, since I_{s} oscillates according to the ac Josephson effect. Therefore, the voltage oscillates with the Josephson frequency f_{J}. As a voltage with such a high frequency cannot be measured, only the time-averaged voltage will be considered in the following discussion. Now, further increasing the energy of the quasiparticles ($T > T_{\mathrm{c}}$ or $V > V_{\mathrm{g}}$) leads to a transition into normal-conducting electrons, which exhibit an ohmic dependence. This behavior can be seen in the typical current-voltage-characteristic (IVC) depicted in figure ???(jj kurve von Alex oder selber messen?).

Real junctions, however, are comprised of two electrodes separated by a thin insulating layer, which represent a parallel plate capacitor with the Al-AlO$_x$ being the dielectric material. Therefore, a junction capacitance C needs to be taken into account. A displacement current I_D will flow as a consequence, given we are in the voltage state. Lastly, thermal and 1/f noise cause a small fluctuating current I_F. All these current channels were defined in the so-called *Resistively and Capacitively Shunted Junction* (RCSJ) *model* ???, which models the total current of a lumped (0-dimensional) junction to a sufficiently high accuracy. A schematic of an effective circuit diagram is shown in figure ???. Combining every current channel leads to the *Basic Junction Equation*, which is defined as

$$I = I_s + I_N + I_D + I_F = I_c \sin(\varphi) + \frac{1}{R(V)} \frac{\Phi_0}{2\pi} \frac{d\varphi}{dt} + C \frac{\Phi_0}{2\pi} \frac{d^2\varphi}{dt^2} + I_F \quad . \tag{1.14}$$

By defining the Josephson coupling energy $U_{J0} = \frac{\hbar I_c}{2e}$ and the normalized currents $i = \frac{I}{I_c}$ and $i_F(t) = \frac{I_F(t)}{I_c}$, equation 1.14 can be rewritten to

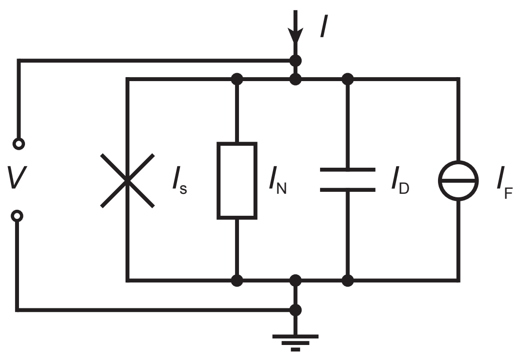

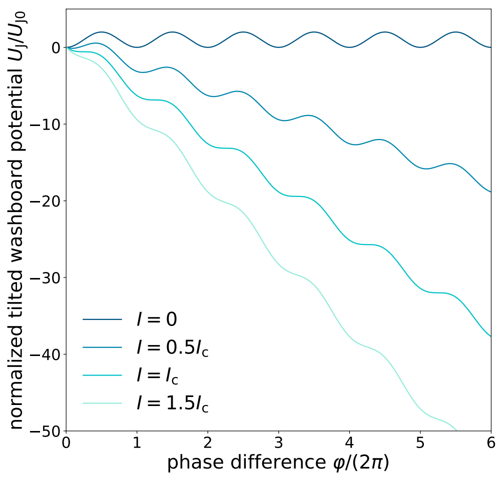

Figure 1.5: Left: Schematic circuit of a lumped Josephson junction with all four current channels connected in parallel. The junction is represented by the cross symbol on the left, marking the supercurrent I_s. The normal current I_N is realized with a resistance R, while the displacement current I_D and the noise I_F need a capacitor C and a current source, respectively. Right: Tilted washboard potential for different currents, ranging from 0 to $1.5I_c$. The tilt increases with the injected current I.

$$\left(\frac{\hbar}{2e}\right)^2 C\frac{\mathrm{d}^2\varphi}{\mathrm{d}t^2}+\left(\frac{\hbar}{2e}\right)^2\frac{1}{R???}\frac{\mathrm{d}\varphi}{\mathrm{d}t}+\frac{\mathrm{d}}{\mathrm{d}\varphi}\left\{U_{\mathrm{J0}}\left[1-\cos\varphi-i\varphi+i_{\mathrm{F}}(t)\varphi\right]\right\}=0 \quad (1.15)$$

.

The expression in the curly brackets represents the potential energy in the system U_{J}, allowing equation 1.14 to be compared to

$$M\frac{\mathrm{d}^2x}{\mathrm{d}t^2}+\eta\frac{\mathrm{d}x}{\mathrm{d}t}+\nabla U=0 \quad (1.16)$$

.

This equation describes a particle with mass M and damping η moving inside the potential U. The mechanical analogue therefore allows us to interpret a *phase particle*, where it's motion corresponds to a change of the gauge-invariant phase difference φ within a potential U_{J}. Consequently, it is attributed with a mass $M = \left(\frac{\hbar}{2e}\right)^2 C$ and damping $\eta = \left(\frac{\hbar}{2e}\right)^2 \frac{1}{R}$. Figure **??** visualizes how this phase particle behaves for different currents I. Given the shape of $U_{\mathrm{J}}(\varphi)$, the potential is referred to as the *tilted washboard potential.*

For $I = 0$, the phase particle will remain within one of the potential minima. As the current increases, however, the potential starts to tilt such that the depth of the minima reduces until it vanishes for $I = I_{\mathrm{c}}$, thus becoming a saddle point. Up until this point, the phase particle can't overcome the potential barrier to move downward, which confirms the second Josephson equation as the phase difference φ should remain constant for $I < I_{\mathrm{c}}$. Further increasing the current and therefore the tilt of the potential causes the phase particle to fall along the potential, resulting in a voltage drop across the junction ($\frac{\partial\varphi}{\partial t} > 0$).

Reversing the current sweep showcases the importance of the particle's mass M and damping η, as they determine if the return path equals the above described current shape or not. For the case of a small mass (small C) and large damping (small R), the phase particle will, due to a lack of momentum, come to a halt as soon as minima reappear in the washboard potential by reducing the current below I_{c}. The current path will therefore remain unchanged as I is reduced back to 0, as shown in figure ???. Such a junction is consequently called an *overdamped* junction.

The other case describes an *underdamped* junction (figure ???) and involves a large mass (large C) and small damping (large R). This allows the phase particle to continue to move downward as it now carries enough momentum to overcome the arising maxima and minima. The finite voltage drop despite the current being below I_{c} is displayed as the steep quasiparticle current curve, which ends with a return current I_{R} that arises with the recapture of the particle in a minimum. This leads to a hysteretic IVC, as depicted in figure ???. I_{R} can be calculated via [Lik86]

$$I_{\mathrm{R}} = \frac{4}{\pi\sqrt{\beta_{\mathrm{C}}}} I_{\mathrm{c}} \quad , \tag{1.17}$$

with β_{C} being the dimensionless Stewart-McCumber parameter ref???, that is used to quantitatively distinguish between both junction types. It is given by

$$\beta_{\mathrm{C}} = \frac{2\pi}{\Phi_0} I_{\mathrm{c}} R^2 C \tag{1.18}$$

with $\beta_{\mathrm{C}} \gg 1$ corresponding to a strongly underdamped junction, whereas $\beta_{\mathrm{C}} \ll 1$ represents a strongly overdamped junction. The junctions developed and produced within the scope of this thesis aim to be overdamped, which is why we take a closer look on the time-averaged voltage for $I > I_{\mathrm{c}}$. Neglecting the noise in equation 1.15, it can be derived to

$$\langle V(t) \rangle = I_{\mathrm{c}} R \sqrt{\left(\frac{I}{I_{\mathrm{c}}}\right)^2 - 1} \quad \text{for} \quad \frac{I}{I_{\mathrm{c}}} > 1 \quad . \tag{1.19}$$

1.2 dc-SQUIDs

1.2.1 Voltage State

1.2.2 Noise

1.3 dc-SQUID Resonances

1.3.1 Parasitic Resonances

1.3.2 Damping Methods

2. Experimental Setup

2.1 Operation of a dc-SQUID

2.1.1 Flux-Locked Loop

2.2 Metallic Magnetic Microcalorimeters

2.3 dc-SQUID Design

Bibliography

[Bar57] J. Bardeen, L. N. Cooper, and J. R. Schrieffer, Theory of Superconductivity, *Phys. Rev.*, **108**(5), 1175–1204, 1957.

[Gin50] V. L. Ginzburg and L. Landau, On the theory of superconductivity, *Zh. Èksper. Teoret. Fiz.*, **20**, 1064–1082, 1950.

[Gro16] R. Gross, A. Marx, and F. Deppe, *Applied Superconductivity: Josephson Effect and Superconducting Electronics*, De Gruyter Textbook Series, Walter De Gruyter Incorporated, 2016.

[Jos62] B. D. Josephson, Possible new effects in superconductive tunnelling, *Physics Letters*, **1**(7), 251–253, 1962.

[Jos65] B. D. Josephson, Supercurrents through barriers, *Advances in Physics*, **14**(56), 419–451, 1965.

[Lik86] K. K. Likharev, *Dynamics of Josephson Junctions and Circuits*, Gordon and Breach, New York, 1986.

[Mei33] W. Meissner and R. Ochsenfeld, Ein neuer Effekt bei Eintritt der Supraleitfähigkeit, *Naturwissenschaften*, **21**(44), 787–788, 1933.

[Tie21] Eite Tiesinga, Peter J. Mohr, David B. Newell, and Barry N. Taylor, Codata recommended values of the fundamental physical constants: 2018, *Rev. Mod. Phys.*, **93**, 025010, 2021.